

Hydration forces and liquid-like layer on the ice/metal interface

This article has been downloaded from IOPscience. Please scroll down to see the full text article.

2007 J. Phys.: Condens. Matter 19 376109

(<http://iopscience.iop.org/0953-8984/19/37/376109>)

View [the table of contents for this issue](#), or go to the [journal homepage](#) for more

Download details:

IP Address: 129.252.86.83

The article was downloaded on 29/05/2010 at 04:40

Please note that [terms and conditions apply](#).

Hydration forces and liquid-like layer on the ice/metal interface

Leonid Daikhin and Vladimir Tsionsky

School of Chemistry, Raymond and Beverly Sackler Faculty of Exact Sciences, Tel-Aviv University, Ramat-Aviv 69978, Israel

E-mail: daikhin@post.tau.ac and tsionsky@post.tau.ac.il

Received 21 February 2007, in final form 16 April 2007

Published 22 August 2007

Online at stacks.iop.org/JPhysCM/19/376109

Abstract

A model to describe the phenomenon of the liquid-like layer is proposed. It is based on the theory of the hydration forces proposed by Gruen and Marcelja (1983 *J. Chem. Soc. Faraday Trans. II* **79** 225), taking into account the influence of ions on the free energy of water. The model was applied to experimental data obtained with the quartz-crystal microbalance, in a study of the liquid-like layer between metal and frozen aqueous electrolytes and between metal and ice.

1. Introduction

The surface properties of any solid differ from its bulk properties. This is the reason for the formation of a liquid-like layer (LLL) at the interface, at temperatures below the bulk melting point (T_m). The formation of this layer is often called a 'premelting'. It is quite likely that the LLL can exist on the surface of many substances [1, 2]. The LLL on ice or between ice and other solids has attracted the greatest attention. The existence of the LLL has been proven by means of different experimental methods, such as mechanical displacement along an ice surface [3–5], photoelectron spectroscopy [6], IR spectroscopy [7, 8], vibrational sum frequency spectroscopy [9–11], nuclear magnetic resonance [12], surface electrical conductivity [13], optical methods [14, 15], atomic-force microscopy [16, 17], the quartz-crystal microbalance [18–21] etc. The experimental results available clearly show that both the thickness (h) of the LLL and degree of disordering of water molecules in it decrease with lowering temperature (increasing supercooling, $\Delta t = T_m - T$). Yet there is a wide range of thickness, from less than 1 nm up to hundreds of nanometres, even at the same temperature. This could be caused by the differences in the properties of the systems studied: ice in contact with water vapour, with metals and with quartz surfaces of different roughness, etc. Another source of such diversity might be the different experimental methods employed to estimate the thickness, which reflect somewhat different properties of the system.

Few theoretical approaches have been proposed to explain the existence of the LLL and the dependence of its properties, primarily its thickness, on temperature. Fletcher [22, 23] considered ice in contact with water vapour. The model is based on the assumption that, at the ice surface, a significant fraction of the molecules is oriented with dipole moments pointing to the gas phase. The reason for this has to do with dipole and quadrupole interactions of the water molecules. This leads to the positive polarization charge of the surface, which is screened by Bjerrum-L defects. The latter is the source of the LLL. The predicted effect for its thickness is approximately $h = 2\text{--}5$ nm at supercooling, $\Delta t = 1$ °C.

The basic premise of the theory of Petrenko and Ryzhkin [24] is the assumption of the existence of a high-density surface charge at ice/vapour and ice/solid interfaces. Whatever the reason for such a surface charge, its presence leads to an increase in the surface density of mobile charge carriers and thus to an increase in the surface conductivity and appearance of the LLL. The calculated thickness of the layer is about 5 nm for supercooling (Δt) of 10 °C. The same authors [25] considered the structure of the proton sublattice of ice at ice/metal interface using the Ginzburg–Landau equation with the boundary condition that describes the presence of the interface. The interactions between protons and substrate can diminish the proton order near the interface and influence the order of the oxygen lattice. The calculated thickness of the LLL at $\Delta t = 3$ °C is less than 1 nm.

The effects of dispersion forces at interfaces between ice and different substrates have been considered by Wilen *et al* [26]. The van der Waals interaction can lead to complete or incomplete melting depending on the type of substrate. Calculation shows that in the case of incomplete melting the layer thickness must be less than 1.5 nm for $\Delta t > 0.1$ °C.

Wettlaufer [27] has examined the influence of an ‘impurity’, referring to low concentrations of a strong electrolyte, on the surface melting of ice. Only at high temperatures ($\Delta t \leq 0.001$ °C) does the classical solute effect (Raoult’s law) dominate melting behaviour. But as the temperature decreases, the van der Waals interaction begins to overcome the influence of the impurity. At low concentration of the ions, Coulomb interactions can effectively compete with van der Waals interactions because of a sufficiently large Debye length.

Henson and Robinson [28] showed that the thickness of the LLL for many substances can be calculated by the universal function of thermodynamic activity. This theory gives, for example, a thickness of approximately 40 nm for the LLL on ice at $\Delta t = 1$ °C.

In [18] we have used, for the first time, the quartz-crystal microbalance to study the LLL at the ice/gold and the frozen electrolyte/gold interfaces. All data are summarized in [21]. The theoretical models mentioned above cannot be applied to the data obtained for one, or both, of the two following reasons: first of all, most models predict very thin LLLs, whereas the LLL thickness observed experimentally could be one or two orders of magnitude larger. Second, these models do not provide a way to take into account the properties of the metal substrate, whereas experiments show that the potential of the metal and adsorption taking place on it could drastically change the thickness of the LLL. In an effort to explain these facts, we propose a model that takes into account the influence of the forces arising from the water structure in the LLL, and the change in the energy of the LLL due to the presence of ions.

2. Experimental data

The quartz-crystal microbalance (QCM) technique is well described in a series of reviews [29–34]. Figure 1 shows a sketch of the instrumental set-up. Usually, the QCM was used in the following configuration: one or both sides of the vibrating quartz plate are in contact with ‘semi-infinite’ gas or liquid medium. In our experiments one side of the QCM was separated from ice (or frozen electrolyte) by an LLL. The existence of this layer

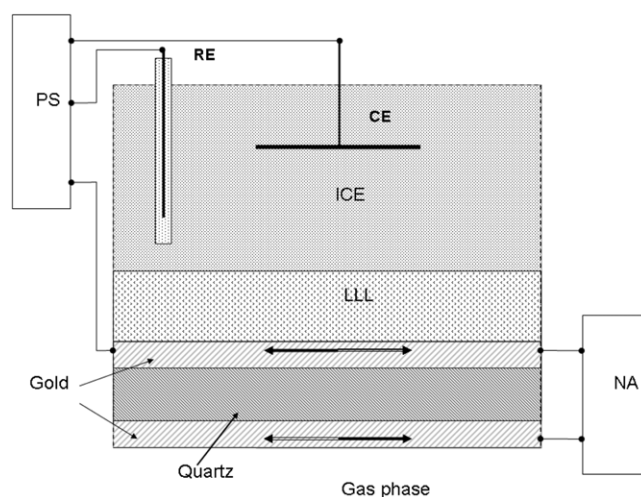


Figure 1. Schematic representation of the set-up. ICE—ice or frozen electrolyte; NA—network analyser (Agilent, E5100A) connected to electrodes (gold) of the QCM; PS—potentiostat (PAR 273) connected to the upper electrode of the QCM, used as a working electrode, and to counter-and reference electrodes (CE and RE, respectively). All dimensions (thickness of the liquid-like layer, LLL, quartz-resonator plate, quartz, etc) are not drawn to scale. In experiments with pure water, PS, RE and CE were not used.

is essential in allowing the QCM to work as a resonator: the layer serves as a ‘lubricant’. Of course its thickness and mechanical properties determine the resonance of the QCM. It can be described by two parameters, directly measured with the network analyser during the experiments: Γ —the width of the resonance peak at its half height—and Δf —the difference between the fundamental frequency measured under given conditions and the fundamental frequency of the unloaded QCM (both sides of the QCM in contact with gas phase He or H₂).

Two models were developed [19] to evaluate the thickness, h , of the LLL, from the experimental data on Γ and Δf . These models consider the movement of the vibrating plate of the QCM, separated by an interlayer (LLL) from an immobile wall (frozen electrolyte). In one model, the LLL is treated as a viscous liquid. This model allows fitting the experimental data only if $\Delta f < 0$. The other model treats the substance in the LLL as a viscoelastic medium and is adaptable to the cases in which Δf is positive or close to zero. Strictly speaking, Δf is not the only parameter that determines the applicability of one or another model. This also depends on the value of Γ (see [18] for a more detailed discussion). Typical data obtained, when studying the LLL with this technique, are shown in figures 2–4. The fact that the response of the QCM in the range of temperatures studied cannot be described by only one assumption concerning the state of substance inside it testifies to the fact that lowering the temperature leads to a strengthening of the interactions between water molecules in the LLL, transforming it from liquid (or liquid-like) into viscoelastic (or solid-like). Under some experimental conditions, the properties of the LLL correspond to some ‘transition’ state and are consistent neither with the liquid-like nor the solid-like states. In such cases it is impossible to calculate h from the response of the QCM. In figures 3 and 4, data corresponding to these cases are marked by crosses.

Calculated values of the thickness of the LLL (h) are shown in figures 2(d) and 4(c). The validity of this way of obtaining the thickness of the LLL was confirmed by simultaneous measurements of h obtained with the QCM and direct measurements of the thickness of the

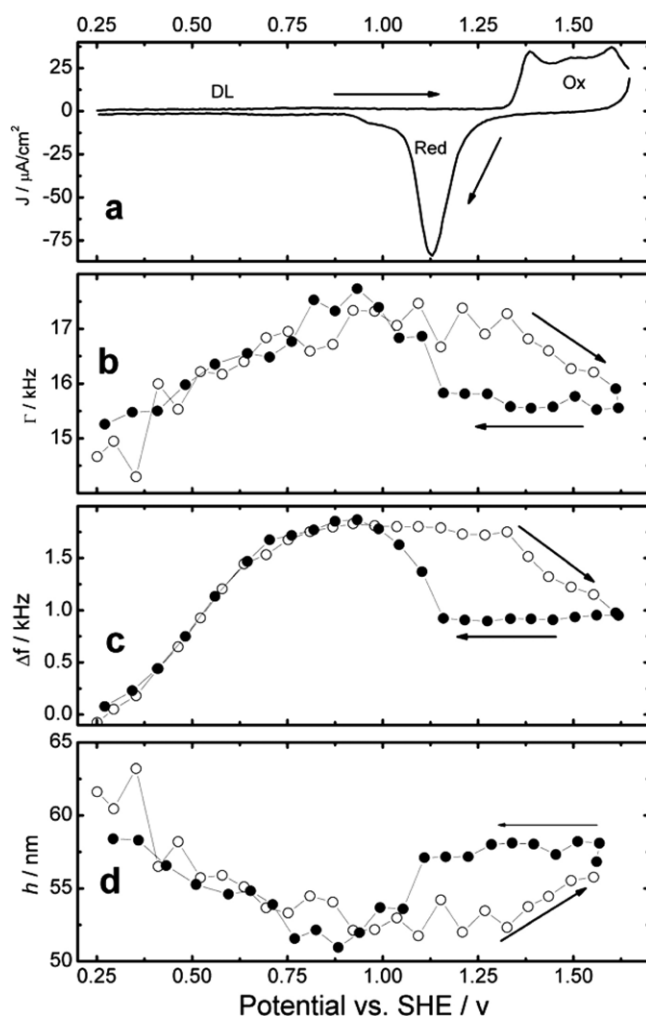


Figure 2. Gold-coated QCM in contact with 0.1 M aqueous solution of HClO_4 at -3.9°C : dependence on potential of (a) current density, J ; (b) width of resonance, Γ ; (c) shift of resonance frequency, Δf , and (d) calculated thickness of the LLL, h . Open and closed circles correspond to different directions of potential scan (10 mV s^{-1}), as shown by the arrows. (From [21].)

LLL with an optic-displacement device [20]: The data obtained by the two techniques are in complete agreement.

Consider the features of the data shown in figure 2, which were obtained at -3.9°C during continuous changes in the electrode potential. The electrochemical behaviour of systems with an LLL is very similar to that usually observed under the same conditions, but at room temperature [35]. In the region marked DL in figure 2(a), only a very small current, corresponding to charging of the electrical double layer, was observed. In this region, h decreases with increasing potential. The increased anodic current in the region marked 'Ox' corresponds to the formation of a surface oxide layer on gold. When the direction of the potential scan is reversed, a cathodic current peak, corresponding to the reduction of this surface oxide, is observed (marked as 'Red'). The variation of h in this region of potentials also shows hysteresis; from this one can conclude that the adsorption of oxygen on the gold

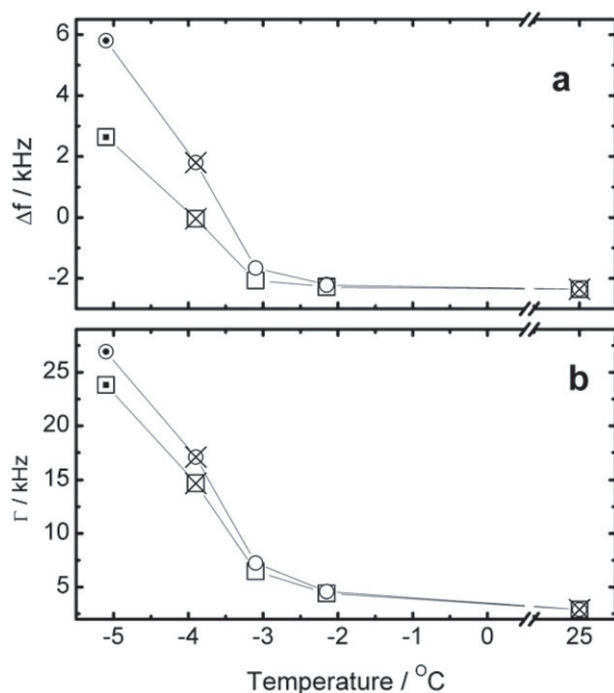


Figure 3. Temperature dependence of (a) shift of resonance frequency, Δf , and (b) width of resonance, Γ , at potentials of 0.3 V (squares) and 0.8 V (circles). Full and blank marks indicate data which could be used to evaluate the thickness of the LLL with the help of models in which the LLL is treated as a viscous liquid and as a viscoelastic medium, respectively. The data marked by crosses correspond to intermediate cases, where neither of the models could be applied.

surface leads to an increase in the thickness of the LLL. Similar variations were obtained at temperatures of -5.1 , -3.1 and -2.15 °C. At all temperatures the cyclic-voltammetry curves are essentially the same. The response of the QCM and h show the same types of dependence, but differ in their absolute values, according to the temperature. Figure 3 summarizes these data showing the temperature dependences of the QCM response for two chosen potentials. At room temperature, the influence of potential and oxygen adsorption on the response of the QCM (as a rule <30 Hz [30, 32]) is fairly negligible on the scale of the graph shown in this figure.

The data shown in figure 4 were obtained with pure water (Milli-Q followed by distillation) with no control of the potential of surfaces of different hydrophilicities (for details see [21]). These data show that the LLL depends strongly on the state of the electrode surface. When the metal surface is made hydrophilic, the LLL could be observed at temperatures only a few tenths of a degree below the melting point. For hydrophobic surfaces, the LLL is observed at much lower temperatures.

Thus, the proposed model of the LLL has to explain the following experimental facts:

- (1) The LLL can be hundreds of nanometres thick even at supercooling of only a few degrees.
- (2) The thickness depends on the potential applied to the metal electrode.
- (3) It is influenced by adsorption of oxygen on the metal surface.
- (4) It depends strongly on the treatment of the metal surface. This means that the thickness of the LLL is determined by the interaction of water with the surface in contact.

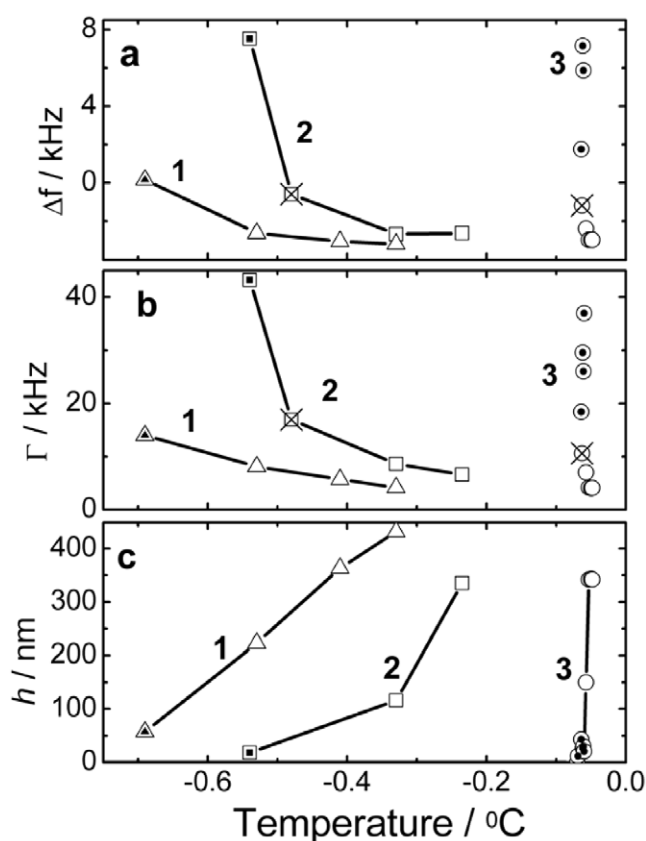


Figure 4. Temperature dependence of (a) the frequency shift, Δf , (b) the width of the resonance, Γ , and (c) the calculated thickness of the LLL, h , obtained in the system of an LLL between ice and bare gold (2), gold modified with cysteamine (hydrophilic surface) (3), and cysteamine and butyl aldehyde (hydrophobic surface) (1).

3. Model

3.1. Hydration forces

The equilibrium structure of bulk liquid water is a random network of hydrogen bonds, many of them strained or broken. The main structural elements of it and the properties of the hydrogen bonds depend on temperature. We consider the layer of water confined between metal and ice surfaces at temperatures below the melting point, T_m , taking into account the electrical potential, which might be applied across the system. In addition, we consider here the case in which the entire potential drop is across the metal/LLL interface; i.e. there is no potential drop across the other interface (LLL/frozen electrolyte). The latter could take place if this interface were permeable to one of the charged species. This seems correct if the electrical conductivity of the system is determined by the mobility of protons, as in acid solutions and pure water systems, which we will discuss below.

We also assume that there is no ordering, leading to non-zero surface polarization, of water molecules near the ice surface; otherwise the interface would melt, according to the concept of Fletcher [22]. In other words, the polarization density ($P(z)$) is zero at the ice/LLL interface

($P(h) = 0$, where h is the LLL thickness). Another situation exists at the metal surface. Chemical interaction between the metal and water molecules leads to some ordering of the latter that might be influenced by the applied potential, i.e. ($P(0) \neq 0$). We consider the LLL to be a structured medium, in which the linear relation between polarization ($P(z)$) and electric field ($E_f(z)$) has been violated. We do not know what the real structure of this layer is. We assume only that the structure of water inside the LLL gives rise to

- (i) the non-parallelism of the electric field and polarization and
- (ii) the existence of decay length of polarization much larger than in liquid water.

In our consideration we follow the work of Gruen and Marcelja [36] in which the polarization in water, described as a structured medium with tetrahedral coordination between molecules, was calculated as the polarization in ice with large concentrations of Bjerrum defects. In the absence of a relation between the configurational polarization, $P(z)$, and the macroscopic electric field in the LLL, $E_f(z)$, these functions have to be obtained from the minimization of the free-energy functional. The free-energy density considered in [36], from the linear approximation, has the form

$$g(z) = \frac{\varepsilon_\infty E_f^2(z)}{8\pi} + \frac{P^2(z)}{2\chi_c} + \frac{\xi^2}{2\chi_c \varepsilon_\infty} \left(\frac{dP(z)}{dz} \right)^2 + \frac{\lambda_D^2}{8\pi \varepsilon_0} \left(\frac{d(\varepsilon_\infty E_f(z) + 4\pi P(z))}{dz} \right)^2. \quad (1)$$

Here, ε_0 and ε_∞ are the low- and high-frequency dielectric constants, respectively, $\chi_c = (\varepsilon_0 - \varepsilon_\infty)/4\pi$ and λ_D is the Debye length. The characteristic length ξ describes the decay of the polarization in the absence of an applied external field. We use the polarization decay length as a parameter that lies in the interval between 0.3 nm in bulk water at room temperature and 33.2 nm in ice [37]. The differential equations for the electric field and the polarization are

$$\lambda_D^2 \left(\varepsilon_\infty \frac{d^2 E_f(z)}{dz^2} + 4\pi \frac{d^2 P(z)}{dz^2} \right) = \varepsilon_0 E_f(z) \quad (2)$$

$$\xi^2 \frac{d^2 P(z)}{dz^2} = \frac{\varepsilon_\infty}{\varepsilon_0} (-\chi_c E_f(z) + P(z)). \quad (3)$$

The solution is determined by the abovementioned boundary conditions:

$$P(0) = P_0, \quad \varepsilon_\infty E_f(0) + 4\pi P(0) = 4\pi\sigma, \quad E_f(h) = 0, \quad P(h) = 0, \quad (4)$$

where σ is the surface-charge density. The solution has the following form:

$$E_f(z) = a \exp(z/\lambda_1) + b \exp(-z/\lambda_1) + c \exp(z/\lambda_2) + d \exp(-z/\lambda_2) \quad (5)$$

$$P(z) = \chi_1 [a \exp(z/\lambda_1) + b \exp(-z/\lambda_1)] + \chi_2 [c \exp(z/\lambda_2) + d \exp(-z/\lambda_2)]. \quad (6)$$

The explicit values of the coefficients a , b , c and d are given in the appendix and

$$\lambda_i = \frac{1}{\sqrt{2}} \left(\lambda_D^2 + \frac{\varepsilon_0}{\varepsilon_\infty} \xi^2 + (-1)^{i+1} \left[\left(\lambda_D^2 + \frac{\varepsilon_0}{\varepsilon_\infty} \xi^2 \right)^2 - 4\xi^2 \lambda_D^2 \right]^{1/2} \right)^{1/2} \quad (7)$$

$$\chi_i = \chi_c \left(1 - \frac{\varepsilon_0 \xi^2}{\varepsilon_\infty \lambda_i^2} \right)^{-1} \quad (8)$$

where $i = 1, 2$. Substitution of solutions (5) and (6) into equation (1) and integration over the layer thickness provides an additional term to the free energy related to the electric field, the polarization and the interaction between them,

$$F(h, P_0, \sigma) = \int_0^h g(z, h, P_0, \sigma) dz - \int_0^\infty g(z, \infty, P_0, \sigma) dz. \quad (9)$$

The difference in chemical potential of the system with a given h and with $h \rightarrow \infty$ as a function of the electric field and polarization can be written as

$$\Delta\mu_P = \frac{1}{\rho_l} \frac{dF(h, P_0, \sigma)}{dh}. \quad (10)$$

3.2. The influence of ions on the free energy of the LLL

The free energy of the LLL, which is in our case an electrolyte, can be calculated by integration of the Gibbs–Duhem equation if we know the ionic free energy. For the mean activity coefficient of a 1–1 electrolyte, we use the simplest expression obtained by Debye and Huckel [38, 39]:

$$\ln(\gamma_{\pm}) = -\frac{A\sqrt{m}}{1+B\sqrt{m}} + bm \quad (11)$$

where $A = \sqrt{2\pi\rho_l N_A} \left(\frac{e^2}{\epsilon_0 kT}\right)^{3/2}$ and $B = a\sqrt{8\pi\rho_l N_A} \frac{e^2}{\epsilon_0 kT}$. Here, N_A , ρ_l , m and a are Avogadro's number, the density of the solvent, molality and the average ionic radius, respectively and b is an empirical parameter. From equation (11) we obtain the expression for the change in the chemical potential of the solvent due to the presence of ions

$$\Delta\mu_{\text{ions}} = 2RT \left[-m(1+bm/2) + \frac{A}{B^3} \left(1 + B\sqrt{m} - \frac{1}{1+B\sqrt{m}} - 2\ln(1+B\sqrt{m}) \right) \right]. \quad (12)$$

We assume, as done in [27], that any change in the thickness of an existing LLL results only from the freezing of water. First of all, this means that the number of ions in the layer is constant and the concentration of ions is inversely proportional to the LLL thickness

$$m = \frac{N_i}{\rho_l h}. \quad (13)$$

Here N_i is the number of ions per unit area. Second, it means that differences in the chemical potentials of frozen and liquid phases can be expressed by taking into account only the latent heat of melting of ice, q_m :

$$\Delta\mu = \frac{q_m}{T_m} (T - T_m). \quad (14)$$

It is clear that equation (13) cannot be used when $h \rightarrow 0$. The observed thickness of the LLL varies in a range of 20–400 nm. Even at these 20-fold ‘compressions’ of the LLL equation (13) could be used as a first approximation.

3.3. Calculation of the thickness of the LLL

From the equilibrium condition (equality of the chemical potentials of the contacting phases: $\Delta\mu = \Delta\mu_P + \Delta\mu_{\text{ions}}$) we obtain the following expression:

$$\frac{1}{\rho_l} \frac{dF(h, P_0, \sigma)}{dh} + \Delta\mu_{\text{ions}}(N_i, h) = \frac{q_m}{T_m} (T - T_m) \quad (15)$$

which permits us to calculate the thickness of the layer as a function of the temperature, the charge density on the metal surface, the surface polarization and the concentration of the electrolyte, $h = h(T, \sigma, P_0, N_i)$. Thus the thickness of the layer is determined by the balance of three forces. The first one is related to the configurational polarization of the LLL (the repulsive hydration force), the second contribution is due to ionic interactions (Debye–Huckel screening effect and Raoult's law) and the third is the thermodynamic force that governs the water/ice bulk equilibrium.

4. Application of the model to experimental data

4.1. The LLL at a frozen electrolyte/metal interface

At this point, we wish to explain how the experimental data, like those shown in figure 2(d), can be applied to equation (15). During an experiment, we obtain three parameters: the thickness of the LLL, h , the temperature, T , and the potential of the metal electrode, E . Now, instead of E , equation (15) contains a function of the surface-charge density, σ . The latter is connected to the electric field and surface polarization through equation (4). As mentioned above, the existence of the LLL practically does not change the shape of the cyclic voltammograms. At all temperatures, they are essentially the same as at room temperature, independent of the presence or absence of the LLL. Moreover, our preliminary measurements of electrochemical-impedance spectroscopy showed that the measured capacitance is also independent of the presence or absence of the LLL. The dependence of σ on potential, E , can be expressed with the use of the experimentally measured double-layer capacitance ($C \approx 70 \mu\text{F cm}^{-2}$) by the following linear relationship:

$$\sigma = C(E - E_{\text{PZC}}), \quad (16)$$

where E_{PZC} is the potential of zero charge of the gold electrode. Clearly, the $\sigma(E)$ dependence is much more complex, and the use of the linear approximation, equation (16), is a simplification. However, at this stage of the research, this simplification seems justified. All previous mathematical treatments leading to equation (15) were also made with the use of linear approximations.

To use equation (15) one needs to make assumptions concerning a few additional parameters.

- (1) The concentration N_i : we assume that the concentration of the electrolyte in a ‘thick’ LLL, the LLL at temperatures near the melting point, is close to the concentration of the initially liquid electrolyte, 0.1 M. For the thickness of this ‘thick’ LLL, we chose 450 nm, the maximum value observed in our experiments. This assumption leads to the value $N_i = 0.045 \text{ mol nm cm}^{-3}$.
- (2) The average ion size, a , from equation (11): we take $a = 5 \text{ \AA}$ as obtained in [40] by fitting the experimental data on the ionic activity coefficient for HClO_4 .
- (3) We can neglect the parameter b from equation (11): at small extent of supercooling when the chemical potential, $\Delta\mu_{\text{ions}}$, determines the thickness of the layer, the concentration is low and term bm in equation (11) is small. The term bm can play an important role only at high concentrations. High concentrations in the LLL can be achieved at high supercooling, when the LLL is thin. However, at small h the contribution of this term of the chemical potential, in comparison with other terms in equation (15), is less important.
- (4) The high-frequency dielectric constant ε_∞ : in the theory of dielectric relaxation, ε_∞ corresponds to the dielectric permeability at frequencies at which the contribution of the orientation polarization of the permanent dipoles of the molecules is very small. It is known from the experiments [41] that for ice $\varepsilon_\infty = 3$. For liquid water it decreases from 6 at 125 °C to 3.9 at 0 °C [42], approaching the value for ice [43]. Another reason for a lower value of ε_∞ could be the influence of ions [42]. In our calculations we use the value $\varepsilon_\infty = 3$.
- (5) The decay length of configurational polarization ξ : its value depends on the structure of the substance. We assume that the substance inside the LLL has a structure intermediate between ice and water. In our calculation, we will use ξ as a parameter with values between 0.3 nm (water [36]) and 30 nm (ice [37]).

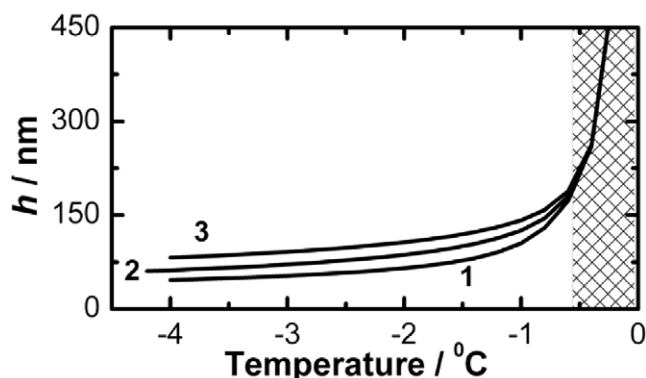


Figure 5. Calculated temperature dependence of the LLL thickness for different decay lengths and surface polarizations at $\sigma = 0$: (1) $\xi = 5$ nm, $P_0 = -0.5P_m$; (2) $\xi = 10$ nm, $P_0 = -0.3P_m$ and (3) $\xi = 10$ nm, $P_0 = -0.5P_m$. $P_m = 32 \mu\text{C cm}^{-2}$ is the maximum value of surface polarization [36].

- (6) It is known [44] that at the potential of zero charge the hydrogen atoms of water molecules are closer to the gold-electrode surface than are the oxygen atoms. We suggest that this orientation also takes place at the gold surface in contact with the LLL, i.e. $P_0 < 0$.

Figure 5 shows typical results of the calculation of h , with the use of equation (15) and the assumptions listed above, for the LLL at a gold electrode in 0.1 M HClO_4 . At small supercooling (crosshatched region), h does not depend on the parameters that characterize polarization (P_0 and ξ). In this region, the existence of the LLL is determined in general by the second term on the left-hand side of equation (15)—by the free energy of the ions (Debye–Huckel screening effect and Raoult’s law). At greater supercooling, the role of polarization becomes crucial. Figure 5 shows that increasing $|P_0|$ and/or ξ result in an increase in the LLL thickness. For this figure, all calculations were made for the case of an uncharged surface ($\sigma = 0$). This means that the electrode potential is equal to E_{PZC} . The shapes of the curves remain qualitatively the same for cases in which $E \neq E_{PZC}$. All the experimental data shown in figures 2 and 3 fall just in the region of strong influence of P_0 and ξ .

Figure 6 shows estimates of the dependence of surface polarization on potential, obtained with the use of experimental data on the behaviour of the LLL at a gold electrode in 0.1 M HClO_4 (figure 2(d)) and similar data at other temperatures (figure 3). We processed only data obtained at potentials corresponding to the so-called ‘double-layer region’, $E < 0.7$ V, where only electrostatic adsorption takes place. The potential of zero charge was taken as 0.2 V versus SHE [45]. The calculated dependences of P_0 on the potential ensure the coincidence of the experimental and theoretical dependences $h(E)$. Figure 6 shows that the higher the temperature the greater the absolute value of the polarization near the electrode. This seems reasonable, because the lower the temperature the more structured must the substance inside the LLL be. At all temperatures, $\partial P_0 / \partial E > 0$. This is also reasonable, since the initially negative polarization diminishes with increase in the positive potential of the metal surface. Here it must be emphasized that this was not fed into the theory, but is only a result obtained with the use of the experimental dependences $h(E)$.

The calculations presented in figure 6 were made under the assumption that ξ is constant at all temperatures and all potentials and is equal to 13 nm. This number was chosen arbitrarily. However, our analysis showed that at $\xi < 10$ nm there is no possibility of correlating the model with the experimental data. Using other values of ξ , different from 13 nm, could lead to other absolute values of P_0 , $\partial P_0 / \partial E > 0$ and $\partial P_0 / \partial T > 0$. Nevertheless, the character of

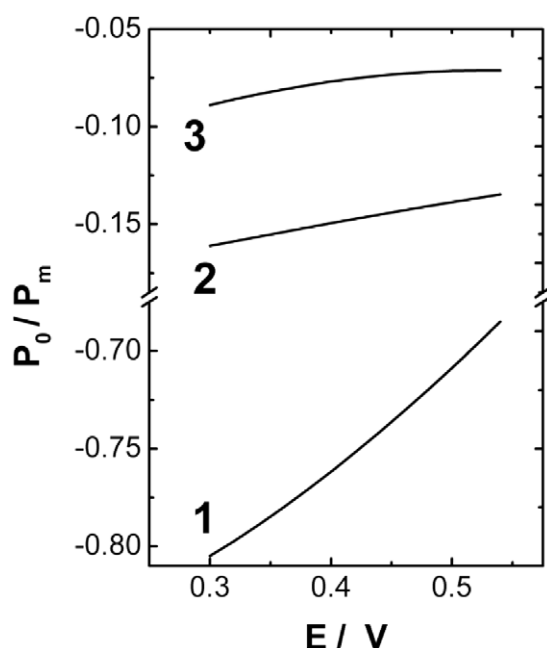


Figure 6. Surface polarization, P_0 , normalized by the maximum value of polarization of water, versus potential, at temperatures of (1) -2.15°C , (2) -3.9°C and (3) -5.1°C .

the dependences shown in figure 6 will remain qualitatively the same. It is reasonable to expect that ξ is also a function of potential and temperature. Intuition suggests that there should be correlation between the changes in ξ and P_0 : the more structured the substance becomes (it does not matter by what means—by changes of temperature or changes of potential) the smaller should $|P_0|$ be and the larger ξ . But at this stage of research we have no concrete information about these correlations and all our calculations serve only to establish a qualitative picture of the phenomena: the decrease in the surface polarization is the main reason for the decrease in the repulsive hydration forces acting between the electrode and ice surface, which leads to the diminishing of the layer thickness.

4.2. LLL at ice/metal interface

Here we wish to correlate the model with the experimental data presented in figure 4, obtained in experiments with pure water in contact with surfaces of different hydrophobicity. We consider pure water an electrolyte containing only H^+ and OH^- ions at concentrations of 10^{-7} M each. Such low concentrations are consistent with a very large Debye length, about 1000 nm, much larger than the observed thickness, h , of the LLL. This means that the polarization decay length must be much smaller than the Debye length, $\xi \ll \lambda_D$. Corresponding calculations of the surface polarization, with the use of equation (15) and data on h (figure 4(b)), show that under these conditions the surface polarization becomes practically independent of ξ .

As in the system containing 0.1 M HClO_4 considered above, the LLL formed from pure water is characterized by a decrease of $|P_0|$ with decreasing temperature. However, in the case of water, the calculated values of $|P_0|$ are remarkably lower. The properties of the LLL in this case are determined mainly by the interplay of ‘thermodynamic’ and hydration forces.

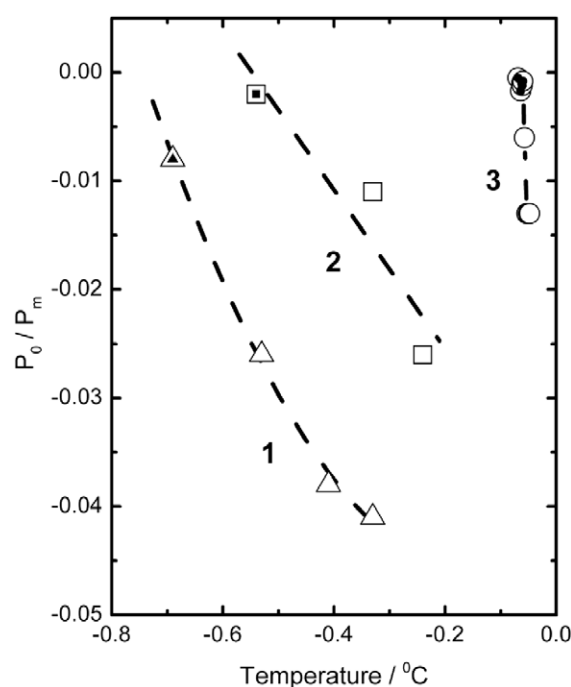


Figure 7. Normalized surface polarization versus temperature for gold surfaces of different hydrophobicities: (1) hydrophobic surface, (2) bare gold and (3) hydrophilic surface. The marks are the same as in figure 3.

The difference in the behaviour of surface polarization of different systems is clearly expressed in figure 7. In the framework of the model proposed above, this difference could be attributed to the different structure of water near surfaces that had undergone different treatments. The structure of water at hydrophilic surfaces sometimes looks like the structure of ice (e.g. hexagonal crystalline ice at the surface of a hydrated protein [46]). It is very probable that the hydrophilic surface, containing NH_2 groups (curve 3), also stimulates creation of a structure with small surface polarization, similar to crystalline ice. The similarity of this surface structure to the structure of ice results in freezing of the LLL under conditions of minimal supercooling. The situation is quite different in the case of a hydrophobic surface. It is well known that water near a hydrophobic surface has a ‘stretched’ 3D structure with an interrupted hydrogen-bond network of water adjacent to the surface (‘dangling hydrogen bonds’ [47]). The preferential orientation of these dangling bonds is responsible for the existence of relatively high surface polarization in liquid water. To decrease this polarization and modify the water structure at a hydrophobic surface into an ice-like structure, in other words to freeze water near the hydrophobic surface, much greater supercooling is needed than in the case of a hydrophilic surface. It is for these reasons that curves 1 and 3 lie in different temperature ranges. It is most likely that the contact between bare gold and water creates neither an ice-like structure, nor one with high surface polarization, but results in some intermediate state.

Effects similar to those shown in figure 7 were observed when contact between a modified surface of silica and ice was studied with vibrational sum frequency spectroscopy [11]: at the hydrophilic (NH_3 dopant) surface of silica, the temperature range of existence of the LLL is very narrow, and vice versa at the hydrophobic surface this temperature interval is much larger.

It has to be noted that the non-treated silica surface shows an intermediate behaviour, similar to the non-treated surface of gold (figure 7, curve 2).

At first glance, it seems strange that calculated values of the surface polarization for a bare gold surface in the system with electrolyte (figure 6) are much higher than for pure water (figure 7). We believe that this is a manifestation of the influence of ions on the structure of water as 'structure-making' agents. This phenomenon was not taken into account in the model. When fitting the model to experimental data obtained with electrolyte, we obtain an apparent value of P_0 as a result of the neglect of the mentioned phenomenon.

4.3. Oxygen adsorption and the LLL

In the section 'the LLL at a frozen electrolyte/metal interface' we restricted our consideration to data obtained in the so-called double-layer region, where only electrostatic adsorption of ions could take place. However, experimental data on the response of the QCM and corresponding estimates of the thickness of the LLL (figure 2) also extend to the potential region where oxygen adsorption takes place. It will be recalled that oxygen adsorption leads to a broadening of the LLL. In this region of potentials, the total measured charge of the electrode consists of the charge expended by the adsorption of oxygen and the surface charge, σ , which is necessary to fit the experimental data to the model. It is impossible to separate these two parts of the total charge that passes through the electrode when the potential is changed. For this reason, the influence of oxygen adsorption on the LLL can be explained only qualitatively: adsorption of oxygen favours preferential orientation of water dipoles, making the water structure less similar to the ice structure and resulting in partial melting and broadening of the LLL.

It should be emphasized that oxygen adsorption and decrease of potential in the 'double-layer' region increase h (figure 2(d)). These effects are in agreement with each other. The presence of oxygen on the surface favours the negative orientation of water dipoles, making P_0 more negative, exactly in the same direction as the decrease in E (figure 5).

4.4. Correlation between models describing the QCM response and the LLL

To extract information on the thickness of the LLL from the data obtained with the QCM technique, we have developed a model [19], which deals only with the mechanical properties of the LLL. This model does not explain either the reasons for the existence of the LLL or the influence of different parameters (temperature, hydrophobicity and potential of the metal surfaces etc). Nevertheless, applying this model leads to the conclusion that, as the temperature decreases, the LLL in a given system is transformed from a liquid (or liquid-like) state to a solid-like state, exhibiting such properties typical to the solid state as elasticity.

The model presented here tries to explain the reasons for the existence of the LLL and its behaviour under the influence of different parameters. It operates with interactions of solvent molecules and ions near the metal/LLL and LLL/ice or frozen electrolyte interfaces. Fitting this model to experimental data showed that the absolute value of surface polarization, $|P_0|$, for all discussed systems decreases with decreasing temperature. Note that all data presented in figures 6 and 7 and initially processed with the model, which considered the substance in the LLL as a viscoelastic medium, have the lowest values of $|P_0|$. This shows correlation between two independent models: low values of $|P_0|$ are typical of well structured, solid systems like ice, naturally possessing elasticity. In the reverse direction, raising the temperature melts the substance inside the LLL, making it less structured, more polarizable, and allowing it to be described as a Newtonian liquid. Unfortunately, there are not enough data to answer the obvious question of whether this transformation goes progressively or it is a phase transition.

5. Conclusion

Experimental data obtained in our laboratory, during a study of the LLL in different systems, showed that the state of the metallic surface (its potential, hydrophobicity, and adsorption taking place on it) could force the processes of melting and freezing of the LLL/ice interface. It is particularly remarkable that both metal/LLL and LLL/ice interfaces could be separated by tens or even hundreds of nanometres. It is clear that these long-range interactions arise from the properties of the substance inside the LLL, probably due to the existence of sufficiently large clusters. The latter could ensure the non-collinearity of the electric and polarization fields and sufficiently large decay length of the polarization.

The model proposed here is based on the theory of hydration forces by Gruen and Marcelja, coupled with generalization of the ideas of Fletcher (dipole and quadrupole interactions and the role of Bjerrum-L defects) and Wettlaufer (electrostatic interaction of ions inside the LLL). The influence of the ions on the free energy of water was taken into account in its simplest form: the expression for the free energy includes Raoult's law and the Debye–Huckel screening effect.

To calculate the thickness of the LLL with the use of the model one needs knowledge of the surface polarization and its dependence on temperature and potential. The lack of this information makes such a calculation impossible. However, the reverse procedure—establishing the surface polarization with the use of experimental data on the thickness of the LLL—evidenced a few aspects that were not *a priori* used in the model.

- (1) As it should, the surface polarization becomes less negative when the potential becomes more positive.
- (2) The surface polarization tends to zero with decreasing temperature. This means that the structure of the substance in the LLL becomes increasingly similar to the structure of ice.
- (3) At a given temperature, the absolute value of the calculated surface polarization, $|P_0|$, is much larger in the case of a hydrophobic surface than in the case of a hydrophilic surface. This is in agreement with what is known about the behaviour of water molecules in the vicinity of these surfaces: a hydrophilic surface creates an ice-like structure while a hydrophobic surface imposes preferential orientation of water dipoles. Here we should also mention the experiments involving oxygen adsorption on a gold surface. Adsorbed oxygen increases the preferential orientation of water dipoles and leads to broadening of the LLL.
- (4) The lowest values of $|P_0|$ were observed only in the cases in which the LLL exhibits the properties of the solid-like state, as revealed from the specific behaviour of the response of the QCM.

At this stage of the research we do not pretend to give a quantitative description of the LLL with the help of the model developed, which clearly needs further refinement and improvement. However, we can state that adding the theory of hydration forces in the description of the LLL gives a consistent qualitative description of its behaviour under the influence of different parameters. It is also evident that there is a lack of experimental data, and the model presented in this paper could guide future experiments, e.g. with electrolytes of different concentrations and ions, differently influencing the structure of water.

Acknowledgment

Financial support for this work by the Israel Science Foundation (grant 174/05) is gratefully acknowledged.

Appendix

The explicit form of the coefficients a , b , c and d :

$$a = \frac{P_0 - \frac{4\pi}{\varepsilon_\infty}(\sigma - P_0)\chi_2}{(\chi_1 - \chi_2)(1 - \exp(2h/\lambda_1))} \quad (\text{A.1})$$

$$b = -a \exp(2h/\lambda_1) \quad (\text{A.2})$$

$$c = -\frac{P_0 - \frac{4\pi}{\varepsilon_\infty}(\sigma - P_0)\chi_1}{(\chi_1 - \chi_2)(1 - \exp(2h/\lambda_2))} \quad (\text{A.3})$$

$$d = -c \exp(2h/\lambda_2). \quad (\text{A.4})$$

References

- [1] Dash J G 2002 *Contemp. Phys.* **43** 427
- [2] Dash J G, Fu H Y and Wettlaufer J S 1995 *Rep. Prog. Phys.* **58** 115
- [3] Gilpin R R 1980 *J. Colloid Interface Sci.* **77** 435
- [4] Churaev N V, Bardasov S A and Sobolev V D 1993 *Colloids Surf. A* **79** 11
- [5] Wilen L A and Dash J G 1995 *Phys. Rev. Lett.* **74** 5076
- [6] Bluhm H, Ogletree D F, Fadley C S, Hussain Z and Salmeron N 2002 *J. Phys.: Condens. Matter* **14** L227
- [7] Sadtchenko V and Ewing G E 2002 *J. Chem. Phys.* **116** 4686
- [8] Sadtchenko V and Ewing G E 2003 *Can. J. Phys.* **81** 333
- [9] Wei X, Miranda P B and Shen Y R 2001 *Phys. Rev. Lett.* **86** 1554
- [10] Richmond G L 2002 *Chem. Rev.* **102** 2693
- [11] Wei X, Miranda P B, Zhang C and Shen Y R 2002 *Phys. Rev. B* **66** 085401
- [12] Ishizaki T, Maruyama M, Furukawa Y and Dash J G 1996 *J. Cryst. Growth* **163** 455
- [13] Khusnatdinov N N, Petrenko V F and Levey C G 1997 *J. Phys. Chem. B* **101** 6212
- [14] Beaglehole D and Nason D 1980 *Surf. Sci.* **96** 357
- [15] Elbaum M, Lipson S G and Dash J G 1993 *J. Cryst. Growth* **129** 491
- [16] Doppenschmidt A and Butt H J 2000 *Langmuir* **16** 6709
- [17] Pittenger B, Fain S C, Cochran M J, Donev J M K, Robertson B E, Szuchmacher A and Overney R M 2001 *Phys. Rev. B* **63** 4102
- [18] Tsionsky V, Zagidulin D and Gileadi E 2002 *J. Phys. Chem. B* **106** 13089
- [19] Tsionsky V, Daikhin L, Zagidulin D, Urbakh M and Gileadi E 2003 *J. Phys. Chem. B* **107** 12485
- [20] Kaverin A, Tsionsky V, Zagidulin D, Daikhin L, Alengoz E and Gileadi E 2004 *J. Phys. Chem. B* **108** 8759
- [21] Tsionsky V, Alengoz E, Daikhin L, Kaverin A, Zagidulin D and Gileadi E 2005 *Electrochim. Acta* **50** 4212
- [22] Fletcher N H 1968 *Phil. Mag.* **18** 1287
- [23] Fletcher N H 1973 *Physics and Chemistry of Ice* ed E Whaley *et al* (Ottawa: Roy. Soc.)
- [24] Ryzhkin I A and Petrenko V F 2002 *Phys. Rev. B* **65** 012205
- [25] Ryzhkin I A and Petrenko V F 2005 *J. Exp. Theor. Phys.* **101** 317
- [26] Wilen L A, Wettlaufer J S, Elbaum M and Schick M 1995 *Phys. Rev. B* **52** 12426
- [27] Wettlaufer J S 1999 *Phys. Rev. Lett.* **82** 2516
- [28] Henson B F and Robinson J M 2004 *Phys. Rev. Lett.* **92** 246107
- [29] Buttry D A 1991 *Electrochemical Interfaces—Modern Techniques for in situ Interface Characterization* ed H D Abruna (New York: VCH) chapter 10
- [30] Buttry D A 1991 *Electroanalytical Chemistry* ed A J Bard (New York: Dekker) chapter 1
- [31] Hillman A R 2003 *Encyclopedia of Electrochemistry* ed A J Bard (Weinheim: Wiley-VCH Verlag GmbH&Co. KGaA) chapter 2.7
- [32] Tsionsky V, Daikhin L, Urbakh M and Gileadi E 2003 *Electroanalytical Chemistry* vol 22, ed A J Bard and I Rubinstein (New York: Dekker) chapter 1
- [33] Johannsmann D 2007 *Piezoelectric Sensors* ed C Steinhilber and A Janshoff (Berlin: Springer) chapter 1
- [34] Urbakh M, Tsionsky V, Gileadi E and Daikhin L 2007 *Piezoelectric Sensors* ed C Steinhilber and A Janshoff (Berlin: Springer) chapter 1
- [35] Tsionsky V, Katz G, Gileadi E and Daikhin L 2002 *J. Electroanal. Chem.* **524** 110
- [36] Gruen D W R and Marcelja S J 1983 *J. Chem. Soc. Faraday Trans. II* **79** 225
- [37] Gruen D W R and Marcelja S J 1983 *J. Chem. Soc. Faraday Trans. II* **79** 211

- [38] Debye P and Huckel E A A 1923 *Phys. Z.* **24** 185
- [39] Huckel E A A 1926 *Phys. Z.* **26** 93
- [40] Robinson R A and Stokes R H 1959 *Electrolyte Solutions* (London: Butterworths)
- [41] Bartie J E, Labbe H J and Whalley E 1969 *J. Chem. Phys.* **50** 4501
- [42] Pottel R 1973 *Water, A Comprehensive Treatise* vol 3, ed F Franks (New York: Plenum)
- [43] Buchner R, Bartel J and Stauber J 1999 *Chem. Phys. Lett.* **306** 57
- [44] Wandlowski T, Ataka K, Pronkin S and Diesing D 2004 *Electrochim. Acta* **49** 1233
- [45] Frumkin A N, Petrii O A and Damaskin B B 1980 *Comprehensive Treatise of Elektrochemistry* ed J O Bockris, B E Conway and E Yeager (New York: Plenum) chapter 5
- [46] Bellissent-Funel M C 2002 *J. Mol. Liq.* **96/97** 287
- [47] Vogler E A 1998 *Adv. Colloid Interface Sci.* **74** 69